Applied Catalysis B: Environmental 202 (2017) 446–453

Contents lists available at ScienceDirect

Applied Catalysis B: Environmental

journal homepage: www.elsevier.com/locate/apcatb

Hydrodeoxygenation of 3-pentanone over bifunctional Pt-heteropoly acid catalyst in the gas phase: Enhancing effect of gold

Olivia Poole, Khadijah Alharbi, Domagoj Belic, Elena F. Kozhevnikova, Ivan V. Kozhevnikov*

University of Liverpool, Department of Chemistry, Liverpool L69 7ZD, UK

ARTICLE INFO

Article history:
Received 10 August 2016
Received in revised form
15 September 2016
Accepted 22 September 2016
Available online 23 September 2016

Keywords:
Hydrodeoxygenation
3-Pentanone
Bifunctional catalysis
Platinum
Gold
Heteropoly acid

ABSTRACT

Hydrodeoxygenation (HDO) of 3-pentanone to yield *n*-pentane was carried out using bifunctional metal-acid catalysis at a gas-solid interface at 40–80 °C and 1 bar H_2 pressure in a fixed-bed microreactor. The bifunctional catalysts studied comprised Pt as the metal component and $Cs_{2.5}H_{0.5}PW_{12}O_{40}$ (CsPW), an acidic Cs salt of Keggin-type heteropoly acid $H_3PW_{12}O_{40}$, as the acid component. The bifunctional HDO pathway included hydrogenation of ketone to secondary alcohol on metal sites followed by dehydration of the alcohol to alkene on acid sites and finally alkene hydrogenation to alkane on metal sites. Addition of gold to the Pt/CsPW was found to increase both catalyst hydrogenation activity (turnover rate at Pt sites) and catalyst stability to deactivation, although the Au alone without Pt was almost totally inert. The enhancement of catalyst performance is suggested to be caused by PtAu alloying. Scanning transmission electron microscopy–energy dispersive X-ray spectroscopy (STEM-EDX) and X-ray diffraction (XRD) analysis of the PtAu/CsPW catalysts indicated the presence of bimetallic PtAu nanoparticles with a wide range of Pt/Au atomic ratios (0.5–7.7).

1. Introduction

Biomass-derived oxygenated organic molecules, such as ketones, carboxylic acids, alcohols, phenols, esters, etc., readily available from fermentation, acid-catalyzed hydrolysis, and fast pyrolysis of biomass, are attractive as renewable raw materials for the environment-friendly production of value-added chemicals and bio-fuels [1,2]. For fuel applications, these oxygenates require reduction in oxygen content to increase their caloric value. Therefore, much current research worldwide is focused on the deoxygenation (hydrodeoxygenation) of renewable organic oxygenates using heterogeneous catalysis [3–11].

Previously, this group and others have reported that platinum on acidic supports, especially, Pt on heteropoly acids (HPA), is a highly active bifunctional metal-acid catalyst for hydrodeoxygenation (HDO) of a wide range of oxygenates in the gas and liquid phases under mild conditions [12–17]. On the other hand, bimetallic PdAu and PtAu catalysts have attracted much attention because of their enhanced performance in comparison to monometallic Pd and Pt catalysts [18–29] (and references therein). Bimetallic enhancement of catalyst performance has been attributed to Au alloying through geometric (ensemble) and electronic (ligand) effects of the constituent elements [28,29]. The ensemble effect, often considered to be more important one [29], can cause structural modifications in the surface metal atom geometry to generate specific isolated surface sites that are highly active for certain reactions. The ligand effect can alter the strength of metal-adsorbate bonds as a result of electronic perturbations of platinum group metal due to heteronuclear metal–metal bond formation, which can also lead to increased catalyst activity in certain reactions. Bimetallic PdAu catalysts have been extensively investigated and employed for many important applications, including, among others, the industrial vinyl acetate synthesis [23,24], low-temperature CO oxidation [25,26], and direct H_2O_2 synthesis from H_2 and O_2 [19]. PtAu bimetallics have been widely used for electrocatalysis in fuel cells [27], but scarcely documented for environment-friendly synthetic applications.

Here, we report the enhancing effect of Au on the gas-phase HDO of a ketone, 3-pentanone, over bifunctional metal-acid catalysts comprising Pt as the metal component and a cesium acidic salt of tungstophosphoric HPA, $Cs_{2.5}H_{0.5}PW_{12}O_{40}$ (CsPW), as the acid component. This catalyst has been shown to be highly efficient in a wide range of HDO reactions [13–15]; it has the highest activity in

* Corresponding author.
E-mail addresses: kozhev@liverpool.ac.uk, I.V.Kozhevnikov@liverpool.ac.uk (I.V. Kozhevnikov).

http://dx.doi.org/10.1016/j.apcatb.2016.09.044
0926-3373/

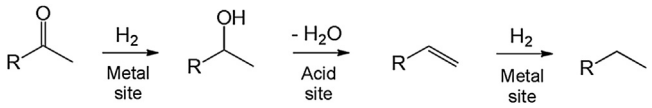

Scheme 1. Ketone hydrodeoxygenation via bifunctional metal-acid catalysis.

the HDO of anisole [15] and aliphatic ketones [13,14] for a gas-phase catalyst system reported so far. The HDO of ketones via bifunctional metal-acid catalysis occurs through a sequence of steps involving hydrogenation of ketone to secondary alcohol on metal sites followed by dehydration of the alcohol to alkene on acid sites and finally hydrogenation of the alkene to alkane on metal sites (Scheme 1) [12–15]. The bifunctional metal-acid catalyzed pathway has been demonstrated to be much more efficient compared to the monofunctional metal-catalyzed ketone-to-alkane hydrogenation [12–14]. It is now demonstrated that modification of the Pt/CsPW catalyst with gold increases the turnover rate of ketone hydrogenation at Pt surface sites and decreases the rate of catalyst deactivation. These effects, however, are dependent on the catalyst formulation and preparation technique. It is suggested that the catalyst enhancement is caused by PtAu alloying. STEM-EDX and XRD analysis of the PtAu/CsPW catalysts indicates the presence of bimetallic PtAu nanoparticles with a wide range of Pt/Au atomic ratios.

2. Experimental

2.1. Chemicals and catalysts

3-Pentanone (98%), $HAuCl_4{\cdot}3H_2O$, H_2PtCl_6 hydrate, $H_3PW_{12}O_{40}$ hydrate, and Darco KB-B activated carbon (150 μm particle size) were all purchased from Sigma-Aldrich. H_2 gas cylinders (>99%) were supplied by the British Oxygen Company.

Cesium tungstophosphate $Cs_{2.5}H_{0.5}PW_{12}O_{40}$ (CsPW) was prepared according to the literature procedure [30] by adding drop-wise the required amount of aqueous solution of cesium carbonate to aqueous solution of $H_3PW_{12}O_{40}$ to afford CsPW as a white precipitate. The material was isolated, oven dried and calcined at 150 °C/10^{-3} kPa for 1.5 h; finally, it was ground to 45–180 μm particle size. The CsPW thus prepared had a single point BET surface area of 133 $m^2\,g^{-1}$, a single point total pore volume of 0.085 $cm^3\,g^{-1}$, and an average pore diameter of 2.5 nm.

CsPW-supported bifunctional metal-acid catalysts were prepared by wet impregnation of CsPW powder with aqueous solutions of H_2PtCl_6 and/or $HAuCl_4$. This involved stirring the aqueous slurry at 50 °C for 2 h followed by rotary evaporation to dryness and reduction with H_2 flow at 250 °C for 2 h. These catalysts had metal loadings between 0.3–6 wt% and hereafter referred to as Pt/CsPW and Au/CsPW. The bimetallic PtAu/CsPW catalysts were prepared similarly; PtAu/CsPW-CI was prepared by co-impregnation, whereas PtAu/CsPW-SI by sequential impregnation of CsPW with H_2PtCl_6 and $HAuCl_4$. The sequential procedure included preparation of Pt/CsPW with reduction by H_2 at 250 °C/2 h followed by impregnation of the Pt/CsPW thus made with $HAuCl_4$ aqueous solution and subsequent reduction (H_2/250 °C/2 h), i.e. in this case, the Pt was treated twice with H_2 at 250 °C. The metal loadings quoted were confirmed by ICP-AES elemental analysis. Supporting Pt and/or Au had little effect on the texture of CsPW, only slightly decreasing the surface area.

Carbon-supported 5%Pt/C and 5%Au/C catalysts were prepared by wet impregnation of Darco KB-B activated carbon with aqueous solutions of H_2PtCl_6 and $HAuCl_4$ at 50 °C for 2 h followed by rotary evaporation to dryness and reduction by H_2 flow as above. Bimetallic PtAu/C catalysts were prepared similarly by wet co-impregnation of the Darco KB-B carbon with H_2PtCl_6 and $HAuCl_4$ (Pt/Au = 1:1 and 1:2 mol/mol); these are hereafter referred to as 5%Pt/5%Au/C-CI and 5%Pt/10%Au/C-CI, respectively. PtAu/C catalysts were also prepared by sequential impregnation either by wet-impregnating the pre-made 5%Pt/C with the required amount of $HAuCl_4$ followed by reduction with H_2 at 250 °C/2 h (referred to as 5%Pt/5%Au/C-SI and 5%Pt/10%Au/C-SI) or the other way around by wet-impregnating the pre-made 5%Au/C with H_2PtCl_6 (referred to as 5%Pt/5%Au/C-SI* and 5%Pt/10%Au/C-SI*). Physically mixed metal-acid bifunctional catalysts 5%Pt/C + CsPW, 5%Au/C + CsPW, 5%Pt/5%Au/C + CsPW, and 5%Pt/10%Au/C + CsPW with 0.5% Pt loading were prepared by grinding a 1:9 w/w mixture of the corresponding two components.

2.2. Techniques

The BET surface area and porosity of catalysts were determined from nitrogen physisorption measured on a Micromeritics ASAP 2010 instrument at −196 °C. Before measurement, the samples were evacuated at 250 °C for 2 h. Powder X-ray diffraction (XRD) patterns of catalysts were recorded on a PANalytical Xpert diffractometer with CuKα radiation (λ = 1.542 Å). XRD patterns were attributed using the JCPDS database. ICP-AES elemental analysis was carried out on a Spectro Ciros optical emission spectrometer. Thermo Flash EA 1112 series analyzer was used to determine carbon content in spent catalysts by combustion chemical analysis.

STEM imaging and EDX analysis of catalysts was carried out on an aberration-corrected JEOL JEM 2100FCs instrument operated at 200 kV, equipped with an EDAX Octane T Optima 60 windowless silicon drift detector. For STEM analysis, the samples were prepared by scooping up the powder catalyst by a TEM grid (holey carbon film on 300 Ni mesh, Agar Scientific) followed by shaking to remove excess material from the grid.

Pt dispersion in the catalysts was measured by hydrogen chemisorption at room temperature in a flow system on a Micromeritics TPD/TPR 2900 instrument using the hydrogen-oxygen titration pulse method described previously [14,15]. The Pt dispersion, D, defined as the Pt fraction at the surface, $D = Pt_s/Pt_{total}$, was calculated assuming the stoichiometry of H_2 adsorption: $Pt_sO + 1.5H_2 \rightarrow Pt_sH + H_2O$ [31,32]. The average diameter of metal particles, d, was obtained from the empirical equation d (nm) = 0.9/D [32]. For some PtAu/CsPW catalysts, the metal particle size was also estimated by XRD using the Scherrer equation, with line broadening assessed as the full width at half maximum intensity (FWHM).

2.3. Catalyst testing

Hydrodeoxygenation of 3-pentanone was carried out in the gas phase in flowing H_2. The catalysts were tested under atmospheric pressure in a Pyrex fixed-bed down-flow microreactor (9 mm internal diameter) fitted with an on-line gas chromatograph (Varian Star 3400 CX instrument with a 30 m × 0.25 mm HP INNOWAX capillary column and a flame ionization detector). The temperature in the reactor was controlled by a Eurotherm controller (±0.5 °C) using a thermocouple placed at the top of the catalyst bed. The ketone was fed by passing H_2 flow controlled by a Brooks mass flow controller through a stainless steel saturator, which held 3-pentanone at 0 °C (ice bath) to maintain the chosen reactant partial pressure of 1.0 kPa (1.0 mol% concentration of 3-pentanone in H_2 flow), unless stated otherwise. The downstream gas lines and valves were heated to 150 °C to prevent substrate and product condensation. The gas feed entered the reactor at the top at a flow rate of 20 mL min^{-1}. The reactor was packed with 0.20 g catalyst powder of 45–180 μm particle size. Typically, the reaction was carried out at a space time W/F = 400 g h mol^{-1}, where W is the catalyst weight (in grams) and F is the inlet molar flow rate

of 3-pentanone (in mol h^{-1}). Prior to reaction, the catalysts were pre-treated in situ for 1 h at the reaction temperature. Once reaction started, the downstream gas flow was analyzed by the on-line GC to obtain reactant conversion and product composition. Product selectivity was defined as moles of product formed per one mole of 3-pentanone converted and quoted in mole per cent. The mean absolute percentage error in conversion and selectivity was ≤5% and the carbon balance was maintained within 95%. Reaction rates (R) were determined as $R = XF/W$ (in mol g_{cat}^{-1} h^{-1}), where X is the conversion of 3-pentanone. Turnover frequencies (TOF) were calculated from the reaction rates using Pt dispersion obtained from hydrogen chemisorption.

3. Results and discussion

3.1. Effect of gold on HDO of 3-pentanone

Previously, it has been found that HDO of aliphatic ketones, including 3-pentanone, over 0.5%Pt/CsPW readily occurs via bifunctional metal-acid catalyzed pathway (Scheme 1) with up to 100% alkane yield in a fixed-bed microreactor under mild conditions (60–100 °C, 1 bar H_2 pressure) [13,14]. Supported Pt/CsPW and physically mixed Pt/C + CsPW catalysts with the same Pt loading exhibit comparable activities in the HDO of aliphatic ketones [14]. The alkane/alcohol product ratio increases with reaction temperature as the result of rate-limiting step change in the HDO process (Scheme 1). 3-Pentanone HDO over 0.5%Pt/CsPW occurs with 80% selectivity to 3-pentanol at 60 °C and 100% selectivity to pentane at 100 °C [14].

In the present work, we examined the effect of Au additives on activity and performance stability of physically mixed and supported bifunctional catalysts comprising Pt and CsPW with different relative amounts of metal and acid components in the HDO of 3-pentanone under kinetically controlled conditions (<100% ketone conversion) in the temperature range of 40–80 °C and W/F = 400 g h mol^{-1}. Gold, indeed, was found to have profound effect on the performance of Pt – CsPW catalysts, subject to catalyst formulation and preparation method.

Addition of Au to Pt/C (Pt/Au = 1:1 and 1:2 atomic ratio) in mixed catalysts Pt/C + CsPW (1:9 w/w, 0.5% Pt loading), did not improve catalyst activity. On the contrary, a decrease in 3-pentanone conversion was observed regardless of catalyst preparation method, i.e., co-impregnation or sequential impregnation. Thus, the unmodified 5%Pt/C + CsPW (1:9 w/w) catalyst gave 70% 3-pentanone conversion with 91% 3-pentanol selectivity at 40 °C, whereas the Au-modified 5%Pt/5%Au/C + CsPW catalyst with the same Pt loading gave 66% and 82%, respectively. Both catalysts showed stable conversion for 4 h on stream (see the Supplementary data, Table S1, Fig. S1 and S2). In the absence of Pt, gold-only catalyst 5%Au/C + CsPW (1:9 w/w) had a negligible activity with only 2% ketone conversion (Table S1). Likewise, CsPW alone was totally inert in this reaction at 40–80 °C.

Next, we looked at a different formulation of the PtAu – CsPW catalysts, with Pt and Au directly supported on the acidic support CsPW. In these catalysts, Pt and Au sites were in close proximity to strong proton sites in CsPW also interacting with the ionic surface of CsPW polyoxometalate, which had profound effect on catalyst performance, i.e., catalyst activity and its resistance to deactivation.

Fig. 1 shows 3-pentanone HDO over unmodified supported catalyst 0.32%Pt/CsPW as well as the corresponding Au-modified catalysts 0.32%Pt/0.36%Au/CsPW-SI and 0.28%Pt/0.35%Au/CsPW-CI prepared by sequential impregnation and co-impregnation of Pt and Au, respectively. The results clearly demonstrate enhancement of catalyst performance by Au additives. First, the co-impregnated catalyst PtAu/CsPW-CI, despite its slightly lower Pt loading, gives a higher ketone conversion as compared to the unmodified Pt/CsPW, while the PtAu/CsPW-SI and Pt/CsPW are almost neck and neck. Second, all three catalysts exhibit deactivation on stream; nevertheless, both Au-modified catalysts deactivate slower than the unmodified Pt/CsPW. It is conceivable that catalyst deactivation is caused by coking originated from oligomerization of alkene intermediates (Scheme 1) on the strong proton sites of CsPW. This is supported by propene oligomerization and coking over supported $H_3PW_{12}O_{40}$ [33,34]. Faster deactivation rate of the supported catalysts in comparison with the mixed ones (PtAu/C + CsPW) can be explained by the close proximity between the Pt and H^+ active sites in the supported catalysts. Also deactivation of the supported catalysts may be increased due to their lower Pt loading and higher Pt dispersion (see below).

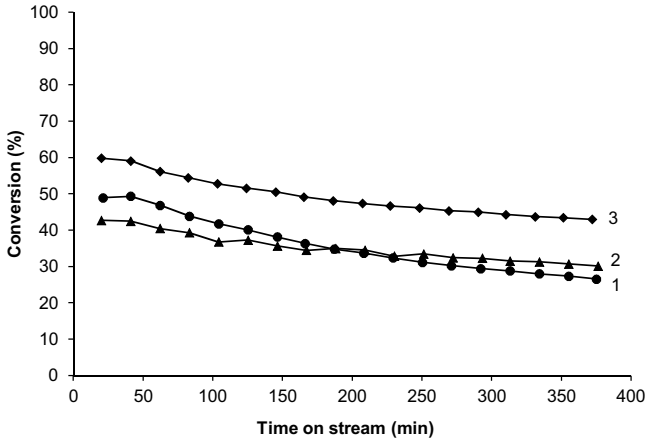

Fig. 1. 3-Pentanone HDO over (1) 0.32%Pt/CsPW, (2) 0.32%Pt/0.36%Au/CsPW-SI and (3) 0.28%Pt/0.35%Au/CsPW-CI (0.20 g catalyst weight, 40 °C, ambient pressure, 1.0% concentration of 3-pentanone in H_2 flow, 20 mL min^{-1} flow rate, catalyst pretreatment at 40 °C/1 h in H_2 flow).

Table 1 presents product selectivity for the supported catalysts, which provides an important insight into the mechanism of Au enhancement. The products contained *n*-pentane, *n*-pentenes (1-pentene, *cis*- and *trans*-2-pentene), and 3-pentanol; no products of skeletal isomerization was observed, which can be explained by low reaction temperature. It should be noted that skeletal isomerization of *n*-hexane over Pt/HPA/SiO_2 catalysts has been reported at 200 °C [35,36]. All three CsPW-supported catalysts, unmodified and Au-modified, had the same 3-pentanol selectivity of 11%. However, pentane/pentene selectivities differed significantly. The Pt/CsPW and PtAu/CsPW-SI, that showed similar performance (Fig. 1), had rather similar selectivities to pentane (56–62%) and pentenes (27–33%). In contrast, the more active co-impregnated catalyst PtAu/CsPW-CI gave significantly more pentenes (52%) at the expense of pentane (37%). This indicates that the Au enhancement of catalyst activity observed for the PtAu/CsPW-CI is largely due to the increased C=O hydrogenation activity, whereas hydrogenation of the alkene C=C double bond appears to be impeded by the Au additives. It is worth noting that the preference of Au catalysts to hydrogenation of the C=O bond over C=C bond has been documented previously, for example, for selective hydrogenation of unsaturated aldehydes to unsaturated alcohols [37,38], despite the opposite thermodynamic preference [37]. Conversely, Pt alone will preferably hydrogenate the C=C bond [37].

Much more profound effect of Au on catalyst stability was observed in the HDO reaction at 80 °C, i.e., under stronger deactivating conditions (Fig. 2). Initially, all three CsPW-supported catalysts exhibited almost 100% 3-pentanone conversion with 100% pentane selectivity. In 6.5 h on stream, the unmodified Pt/CsPW lost 70% of its initial activity and its pentane selectivity reduced to 95% in favor

Table 1
HDO of 3-pentanone over Pt/CsPW and PtAu/CsPW.[a]

Catalyst	Conv.[b]	Selectivity (%)				
	(%)	pentane	1-C_5H_{10}	trans-2-C_5H_{10}	cis-2-C_5H_{10}	3-pentanol
0.32%Pt/CsPW	36	56	<1	15	18	11
0.32%Pt/0.36%Au/CsPW-SI	35	62	<1	13	14	11
0.28%Pt/0.35%Au/CsPW-CI	49	37	<1	23	29	11

[a] Reaction conditions: 0.20 g catalyst weight, 40 °C, ambient pressure, 1.0% concentration of 3-pentanone in H_2 flow, 20 mL min^{-1} flow rate, catalyst pre-treatment at 80 °C/1 h in H_2 flow, 6 h time on stream.
[b] Average 3-pentanone conversion over 6 h time on stream.

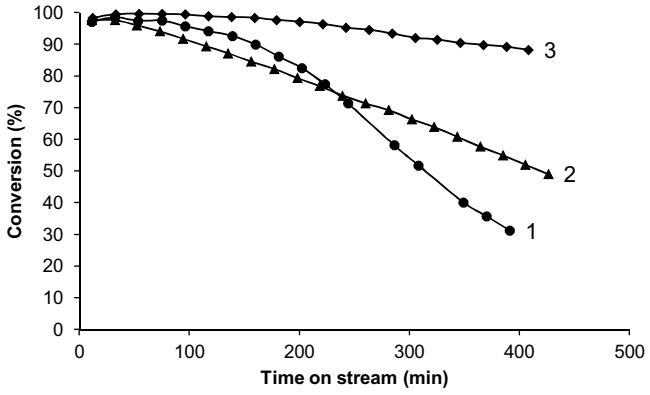

Fig. 2. 3-Pentanone HDO over (1) 0.32%Pt/CsPW, (2) 0.32%Pt/0.36%Au/CsPW-SI and (3) 0.28%Pt/0.35%Au/CsPW-CI (0.20 g catalyst weight, 80 °C, ambient pressure, 1.0% concentration of 3-pentanone in H_2 flow, 20 mL min^{-1} flow rate, catalyst pre-treatment at 80 °C/1 h in H_2 flow).

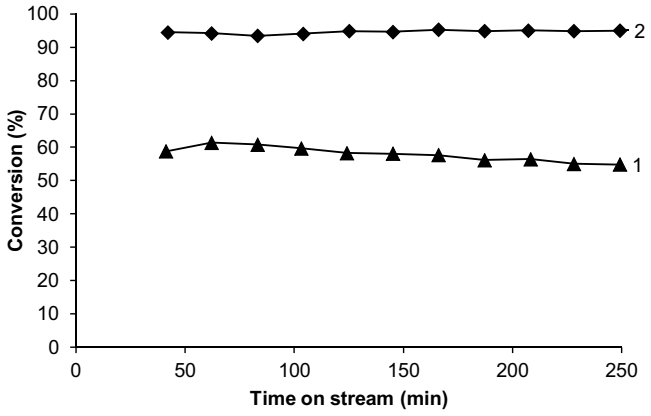

Fig. 3. 3-Pentanone HDO over (1) 5.4%Pt/CsPW and (2) 5.3%Pt/3.3%Au/CsPW-CI diluted 1:7 w/w by SiO_2 to 0.7% Pt loading (0.20 g catalyst weight, 40 °C, ambient pressure, 1.0% 3-pentanone concentration in H_2 flow, 20 mL min^{-1} flow rate, catalyst pre-treatment at 40 °C/1 h in H_2 flow).

of 3-pentanol formation. The Au-modified PtAu/CsPW-SI prepared by sequential impregnation lost half of its activity (49% conversion and 98% pentane selectivity at 7 h time on stream). The best performance stability was displayed by the co-impregnated catalyst PtAu/CsPW-CI, which showed 88% conversion and 100% pentane selectivity after 7 h on stream. Combustion analysis of spent catalysts indicated that catalyst deactivation rate was in line with the amount of coke formed, which decreased in the order (C content, %): 2.6 (Pt/CsPW) >2.5 (PtAu/CsPW-SI) >2.2 (PtAu/CsPW-CI).

Further, the effect of Au was tested in a series of bifunctional metal-acid catalysts with various relative amounts of metal (Pt) and acid (CsPW) components to compare unmodified Pt/CsPW catalysts with Au-modified co-impregnated PtAu/CsPW-CI catalysts that showed greater enhancement of catalyst performance.

Fig. 3 shows the HDO of 3-pentanone at 40 °C over catalysts with reduced acid function. These catalysts comprised 5.4%Pt/CsPW and 5.3%Pt/3.3%Au/CsPW-CI diluted 1:7 w/w by SiO_2 (0.7% Pt loading). These reactions predictably yielded 3-pentanol as the main product (95–97% selectivity, Fig. S3) due to slowing down the alcohol dehydration step (Scheme 1). The unmodified Pt/CsPW catalyst gave 58% average ketone conversion over 4 h on stream, with a slight catalyst deactivation. The Au-modified catalyst, PtAu/CsPW-CI, again demonstrated significant enhancement of catalyst activity to exhibit a stable 95% ketone conversion.

The reaction with similar catalysts, but with increased acid function, is shown in Fig. 4. In this case, 5.8%Pt/CsPW and 5.6%Pt/4.3%Au/CsPW-CI catalysts were diluted 1:19 w/w with CsPW (0.3% Pt loading). As a result, reaction selectivity changed dramatically to yield mainly C_5 hydrocarbons, i.e., pentane and pentenes (91% selectivity, C_5H_{12}/C_5H_{10} = 16 mol/mol for Pt/CsPW and 86%, C_5H_{12}/C_5H_{10} = 6.6 for PtAu/CsPW-CI). The increased catalyst acidity led to an increase in catalyst deactivation rate (cf. Fig. 3), and again the Au enhancement of catalyst stability is clearly visible. Along with reducing the rate of catalyst deactivation, addition of Au increased the average ketone conversion from 21% for

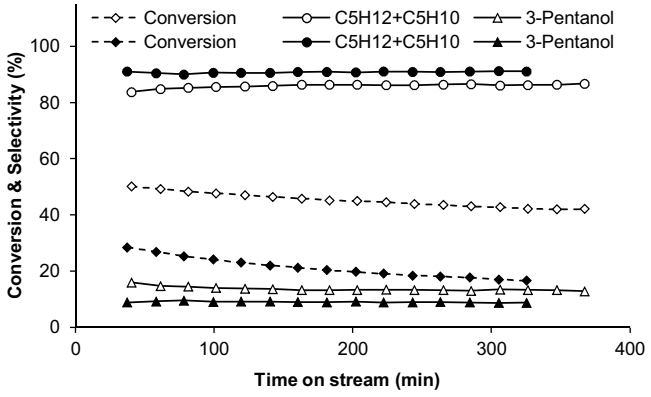

Fig. 4. 3-Pentanone HDO over 5.8%Pt/CsPW (solid markers) and 5.6%Pt/4.3%Au/CsPW-CI (open markers) diluted 1:19 w/w by CsPW to 0.3% Pt loading (0.20 g catalyst weight, 40 °C, ambient pressure, 1.0% concentration of 3-pentanone in H_2 flow, 20 mL min^{-1} flow rate, catalyst pre-treatment at 40 °C/1 h in H_2 flow).

Pt/CsPW to 45% for PtAu/CsPW-CI over 6 h time on stream (Fig. 4). Again, from the pentane/pentene product ratio, the preference of PtAu catalyst for the C=O over C=C hydrogenation can be clearly seen, as compared to the unmodified Pt catalyst (C_5H_{12}/C_5H_{10} = 16 and 6.6 mol/mol for Pt/CsPW and PtAu/CsPW-CI, respectively). It should be noted that the Au-only catalyst, 2.6%Au/CsPW + CsPW (1:19 w/w), showed only negligible activity (~1% ketone conversion).

Finally, the effect of Au was examined under very strong deactivating conditions at 80 °C using bifunctional catalysts with greatly increased acid function over metal function. In this case, 5.8%Pt/CsPW and 5.6%Pt/4.3%Au/CsPW-CI were diluted by CsPW 1:79 w/w to 0.07% Pt loading. The results are shown in Fig. 5. Initially, in this system pentane was the only product (~100%

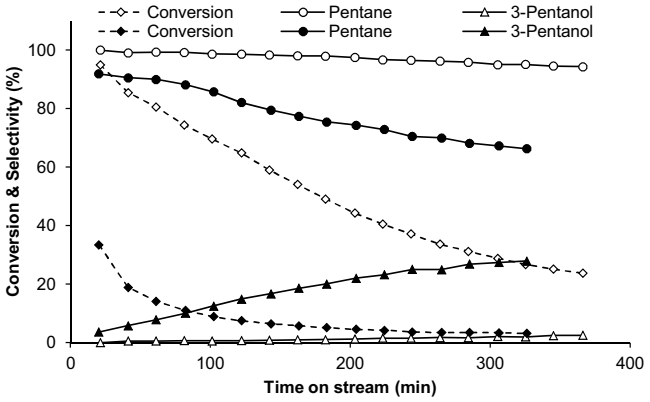

Fig. 5. 3-Pentanone HDO over 5.8%Pt/CsPW (solid markers) and 5.6%Pt/4.3%Au/CsPW-CI (open markers) diluted 1:79 w/w by CsPW to 0.07% Pt loading (0.20 g catalyst weight, 80 °C, ambient pressure, 1.0% concentration of 3-pentanone in H_2 flow, 20 mL min^{-1} flow rate, catalyst pre-treatment at 80 °C/1 h in H_2 flow).

selectivity). In the course of reaction, the unmodified Pt/CsPW was severely deactivated losing practically all its activity in 6 h on stream. Its selectivity was also changed to form 3-pentanol at the expense of pentane. The Au-modified catalyst was also deactivating, but at a much slower rate, with its pentane selectivity only slightly changing from 100 to 94%. The amount of coke formed in the Au-modified catalyst (2.8%) was smaller than in the Pt/CsPW (3.1%), which is in agreement with the stability of these catalysts.

Therefore, the modification of Pt/CsPW catalyst with gold increases its activity (ketone conversion) in the HDO of 3-pentanone and decreases the rate of catalyst deactivation, although the gold itself is inert in this reaction. The activity enhancement also indicates the preference of the PtAu/CsPW catalysts toward hydrogenation of C=O bond over C=C bond in comparison with the unmodified Pt/CsPW. The Au enhancement appears to be strongly dependent on catalyst formulation as well on the catalyst preparation method. Carbon-supported Pt and Au physically mixed with CsPW solid acid failed to show any enhancement, whereas the metals directly supported onto CsPW did display the enhancement effect. This indicates importance of close proximity between metal and proton active sites in the bifunctional metal-acid catalysts. This might also indicate a special role of the acidic CsPW polyoxometalate support, however there is no direct evidence for that as yet. PtAu catalysts prepared by co-impregnation of metal precursors showed stronger enhancement effect in comparison with the catalysts prepared by sequential impregnation. It is conceivable that Pt-Au alloying was the cause of the enhancement of catalyst performance as the result of the ensemble and ligand effects of Au on the Pt active sites [28,29]. In this respect, the co-impregnation is expected to be more favorable for Pt-Au alloying than the successive impregnation.

3.2. Catalyst characterization

This includes investigation of metal nanoparticles in Pt/CsPW and PtAu/CsPW catalysts by X-ray powder diffraction (XRD), scanning transmission electron microscopy–energy dispersive X-ray spectroscopy (STEM-EDX) and H_2 chemisorption. The STEM-EDX and XRD analysis of the PtAu/CsPW catalysts indicated the presence of PtAu bimetallic nanoparticles, which may be the cause of catalyst performance enhancement.

Supported bimetallic catalysts, while preferred for practical use, have a drawback, which is the lack of homogeneity of metal nanoparticles regarding their composition, size, and shape [29]. The method of preparation of the CsPW-supported PtAu catalysts

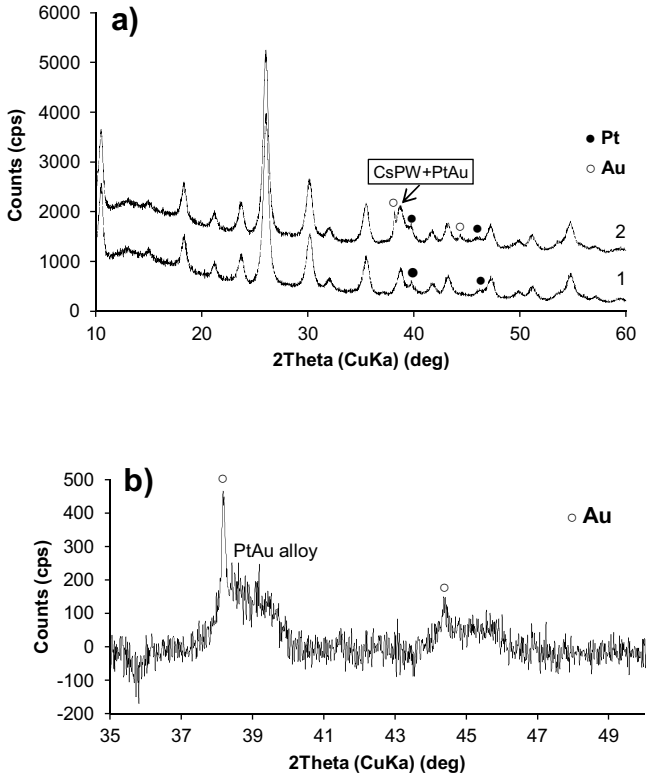

Fig. 6. XRD patterns: (a) 5.8%Pt/CsPW (1) and 5.6%Pt/4.3%Au/CsPW-CI (2); (b) close-up normalized difference (2)-(1) XRD pattern revealing a broad [111] fcc PtAu alloy peak in the range 38–40° and possibly a weaker [200] PtAu alloy peak in the range 44–46°.

chosen in this work involves formation of metal nanoparticles at a gas-solid interface upon reduction of a solid pre-catalyst with H_2 at 250 °C. This would favor formation of supported PtAu alloys of a random composition together with various Pt-alone and Au-alone nanoparticles, rather than specific core-shell bimetallics often formed in solution in the presence of a protective agent preventing aggregation [29].

X-ray powder diffraction (XRD) has been widely used for the characterization of supported Au alloy catalysts [29]. XRD patterns for unmodified 5.8%Pt/CsPW and Au-modified 5.6%Pt/4.3%Au/CsPW-CI catalysts are shown in Fig. 6a. These are dominated by the well-known bcc pattern of crystalline CsPW [39] and also clearly display the fcc pattern of Au (38.2° [111] and 44.4° [200]) and Pt (39.8° [111] and 46.2° [200]) metal nanoparticles. As expected, this indicates coexistence of Pt-alone and Au-alone particles and possibly PtAu bimetallic particles with diffraction pattern falling in between the corresponding diffractions of the pure metals [29]. The latter, however, is obscured by the intense pattern of CsPW in Fig. 6a. Nevertheless, the normalized difference XRD (Fig. 6b) shows a broad diffraction peak in the range of 38–40° between the diffractions of pure Pt and Au, which could be attributed to PtAu alloys. It should be noted that Pt peaks appear broader than Au peaks (Fig. 6a), which indicates higher dispersion of Pt particles. Accurate analysis of metal particle size is difficult due to the dominance of the CsPW pattern. Rough estimate from the [111] peaks using the Scherrer equation gave 60 and 30 nm volume-average particle size for Au and Pt, respectively, which may be biased toward larger metal particles.

Scanning transmission electron microscopy (STEM) and energy dispersive X-ray spectroscopy (EDX) have been used extensively for the characterization of PdAu [19,22,29] and PtAu [27] nanoparticles. Fig. 7 shows the high-angle annular dark field (HAADF)

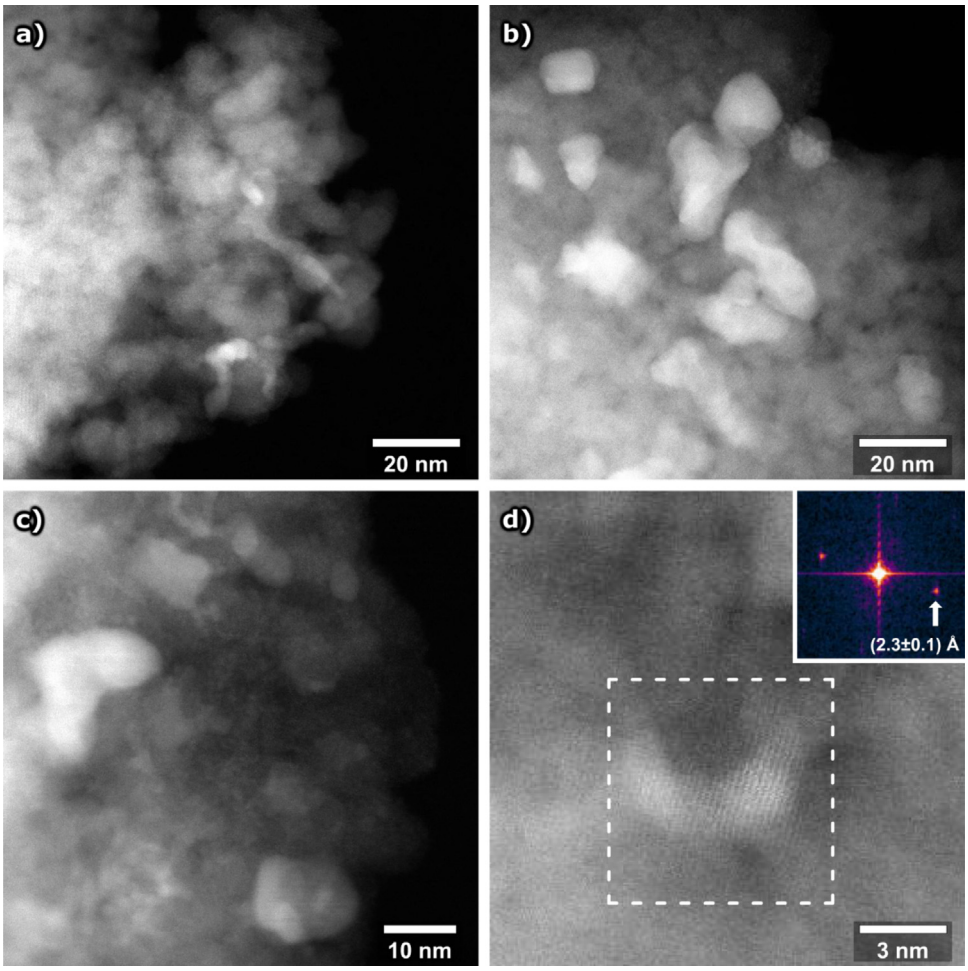

Fig. 7. HAADF-STEM images of catalyst samples, showing metal nanoparticles as bright spots: (a) 5.8%Pt/CsPW, (b) 2.6%Au/CsPW, and (c) 5.6%Pt/4.3%Au/CsPW-CI; a high-resolution image (d) of sample 5.6%Pt/4.3%Au/CsPW-CI, with fast Fourier transform (FFT) of the marked area given in the inset, revealing the crystalline structure of metal nanoparticle.

STEM images of the three catalysts 5.8%Pt/CsPW, 2.6%Au/CsPW and 5.6%Pt/4.3%Au/CsPW-CI with metal nanoparticles indicated as bright spots on the darker background. As gold, platinum and tungsten all have similar atomic number Z (74, 78, and 79 for W, Pt, and Au, respectively), the strong background of CsPW containing 70 wt% of W in these catalysts makes it difficult to discern smaller Pt and Au particles from the Z-contrast HAADF images. Due to this, no accurate determination of the metal particle size distribution could be made. Fig. 7a (sample 5.8%Pt/CsPW) shows platinum particles with a size of ≤12 nm. Fig. 7b (sample 2.6%Au/CsPW) shows oval shaped gold particles sized up between 4 and 25 nm, with an average gold particle size estimated to be ≤10 nm. Particles of a similar size and shape can be seen in Fig. 7c (sample 5.6%Pt/4.3%Au/CsPW-CI), which is suggestive of a PtAu alloying on the catalyst surface (see the EDX analysis below). It can be seen that individual nanoparticles in this catalyst exhibit well-defined low-index facets with a lattice spacing of 2.3 ± 0.1 Å consistent with [111] interplanar distances in fcc Au or Pt (Fig. 7d).

The EDX analysis of a large number of metal nanoparticles in the 5.6%Pt/4.3%Au/CsPW-CI catalyst showed that all these particles contained both platinum and gold in different Pt/Au atomic ratios varying from 0.5 to 7.7 (Figs. 8 and S4 in the Supplementary data). This may indicate PtAu alloying in this catalyst. EDX elemental mapping showed that Pt and Au maps covered the same areas of PtAu/CsPW catalyst particles (Fig. S5), indicating formation of a non-uniform PtAu particles, with local variations in Pt/Au atomic ratio.

Table 2
H_2/O_2 titration of catalysts.

Catalyst[a]	H_2/Pt_{total} (mol/mol)	D[b]	d[c] (nm)
0.32%Pt/CsPW	0.91 ± 0.13	0.61 ± 0.09	1.5
0.28%Pt/0.35%Au/CsPW-CI[d]	0.83 ± 0.09	0.55 ± 0.06	1.6
0.32%Pt/0.36%Au/CsPW-SI[e]	0.45 ± 0.09	0.30 ± 0.06	3.0
5.8%Pt/CsPW	0.28 ± 0.07	0.19 ± 0.05	4.7
5.6%Pt/4.3%Au/CsPW-CI[d]	0.26 ± 0.03	0.17 ± 0.02	5.3
2.6%Au/CsPW	0[f]		≤10
CsPW[g]	0[f]		

[a] Metal loadings obtained from ICP-AES analysis.
[b] Pt dispersion determined as an average from three H_2/O_2 titration measurements assuming negligible H_2 adsorption on gold.
[c] Metal particle diameter: for Pt from the equation d (nm) = 0.9/D, for Au from STEM.
[d] Catalysts prepared by co-impregnation of H_2PtCl_6 and $HAuCl_4$ followed by reduction with H_2 at 250 °C/2 h.
[e] Catalyst prepared by sequential impregnation of H_2PtCl_6 then $HAuCl_4$, with Pt(IV) reduced to Pt(0) with H_2 at 250 °C/2 h prior to $HAuCl_4$ impregnation, then the $Pt^{0}Au^{III}$/CsPW was reduced with H_2 at 250 °C/2 h.
[f] No H_2 adsorption observed.
[g] Single point BET surface area, 133 m^2g^{-1}; single point total pore volume, 0.085 cm^3g^{-1}; average pore diameter, 2.5 nm.

An accurate assessment of metal dispersion was obtained from hydrogen adsorption. Table 2 shows the results of H_2/O_2 titra-

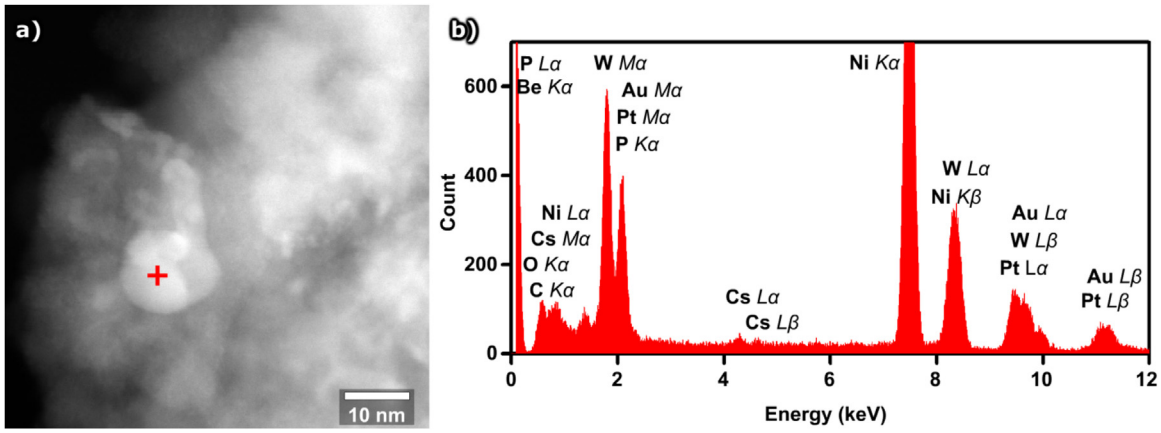

Fig. 8. (a) HAADF-STEM image of 5.6%Pt/4.3%Au/CsPW-CI catalyst sample, with the cross on a 12 nm PtAu nanoparticle marking the spot where EDX analysis was performed; (b) the corresponding EDX spectrum, revealing the atomic ratio Pt/Au = 7.7, indicating that the probed PtAu nanoparticle is Pt-rich.

Table 3
Turnover rates for Pt/CsPW and PtAu/CsPW catalysts at 40 °C.[a]

Catalyst	D[b]	d[c] (nm)	Initial conversion	Initial rate ($mol\,g_{cat}^{-1}h^{-1}$)	TOF (h^{-1})
0.32%Pt/CsPW	0.61	1.5	0.490	$1.23{\cdot}10^{-3}$	0.63
0.28%Pt/0.35%Au/CsPW-CI	0.55	1.6	0.599	$1.50{\cdot}10^{-3}$	0.97
0.32%Pt/0.36%Au/CsPW-SI	0.30	3.0	0.427	$1.07{\cdot}10^{-3}$	1.1
5.8%Pt/CsPW	0.19	4.7	0.286	$1.43{\cdot}10^{-2}$	1.3
5.6%Pt/4.3%Au/CsPW-CI	0.17	5.3	0.502	$2.51{\cdot}10^{-2}$	2.6
5.6%Pt/4.3%Au/CsPW-CI[d]	0.17	5.3	0.225	$2.25{\cdot}10^{-2}$	2.3

[a] Calculated form the results shown in Figs. 1 and 4 obtained at 1.0% concentration of 3-pentanone in H_2 flow.
[b] Pt dispersion (Table 2).
[c] Pt particle diameter (Table 2).
[d] At 2.0% concentration of 3-pentanone in H_2 flow, other conditions as in Fig. 4.

tion of CsPW-supported Pt and PtAu catalysts, which was carried out at room temperature by the pulse method in flow system (an example of H_2/O_2 titration is shown in Fig. S6). Under such conditions, CsPW did not adsorb any hydrogen, in agreement with the previous report [40]. No hydrogen adsorption was observed on the Au/CsPW either, which is also in agreement with the literature [18,31,41]. Hence the adsorption of H_2 observed on the PtAu catalysts was attributed entirely to platinum. Pt dispersion, D, in 0.32%Pt/CsPW was found to be 0.61 and predictably reduced to 0.19 in 5.8%Pt/CsPW, which corresponds to a Pt particle size of 1.5 and 4.7 nm in these catalysts, respectively. The PtAu/CsPW catalysts prepared by co-impregnation showed a small reduction trend in Pt dispersion in comparison with the unmodified Pt/CsPW catalysts, although the difference was within the experimental error. This may be explained by PtAu alloying. Notably, the Pt dispersion in the 0.32%Pt/0.36%Au/CsPW-SI catalyst prepared by sequential Au-after-Pt impregnation dropped significantly down to 0.30 (Table 2). This may be the reason for the less efficient performance of this catalyst as compared to the co-impregnation catalyst 0.28%Pt/0.35%Au/CsPW-CI (see above).

With the Pt dispersion obtained, we can now calculate turnover rates (TOF) for Pt and PtAu catalysts and estimate the effect of gold on the intrinsic activity of Pt surface sites. As the gold alone was practically inactive, the catalyst activity can be attributed entirely to the Pt sites. Previously, it has been shown that ketone HDO over Pt/CsPW catalyst is zero order in ketone and near first order in Pt loading [13]. The HDO of 3-pentanone over 5.6%Pt/4.3%Au/CsPW-CI was also found to be zero order in ketone, as the initial reaction rate practically did not change upon increasing ketone concentration in the feed from 1.0 to 2.0% (Table 3, last two entries). This means that 3-pentanone conversion is equivalent to the reaction rate constant, which allows obtaining TOF values from non-differential conversions. Table 3 shows the TOF values thus obtained for Pt/CsPW and PtAu/CsPW catalysts at 40 °C, which were calculated from the results presented in Figs. 1 and 4 using initial 3-pentanone conversion (varied between 29 and 60%) and Pt dispersion from Table 2. These results show that the turnover rate at Pt sites in the gold-free Pt/CsPW catalysts is weakly dependent on Pt dispersion, decreasing 2-fold with a 3-fold increase in the Pt dispersion within the range of 0.32–5.8% Pt loading. Gold additives increase the intrinsic activity of Pt surface sites. More specifically, addition of Au to Pt/CsPW in a Pt/Au molar ratio of about 1:1 and a gold loading of 0.35–4.3% increases the turnover rate at the Pt sites almost 2-fold regardless of the Pt particle size. This may indicate that Au enhancement of Pt hydrogenation activity is structure insensitive, as may be expected for catalytic hydrogenation [42].

4. Conclusions

Here, we have demonstrated the enhancing effect of gold on activity and stability of Pt/CsPW bifunctional metal-acid catalyst in hydrodeoxygenation (HDO) of 3-pentanone. Addition of gold increases the turnover rate of 3-pentanone HDO at Pt sites. The bimetallic catalyst PtAu/CsPW shows the preference of C=O over C=C bond hydrogenation in comparison with the unmodified Pt/CsPW catalyst. The Au enhancement has been found to be dependent on catalyst formulation as well as catalyst preparation method. STEM-EDX and XRD analysis indicates the presence of bimetallic nanoparticles with a wide range of Pt/Au atomic ratios in the PtAu/CsPW catalysts. The catalyst enhancement can be attributed to the two previously documented Au alloy effects, i.e., ensemble and ligand effects [28,29]. These effects can modify the geometry and electronic state of Pt active sites to enhance their activity toward C=O bond hydrogenation and reduce catalyst poisoning.

Overall, the results obtained confirm the view that the addition of Au is a promising methodology to enhance the HDO of biomass-derived feedstock using platinum group metal catalysts [28,29].

Acknowledgements

We thank Dr T. Heil from Nanoinvestigation Centre, University of Liverpool for assistance with the STEM. Dr D. Belic acknowledges funding through ERC Advanced Grant "PANDORA" No. 108269.

Appendix A. Supplementary data

Supplementary data associated with this article can be found, in the online version, at http://dx.doi.org/10.1016/j.apcatb.2016.09.044.

References

[1] A. Corma, S. Iborra, A. Velty, Chem. Rev. 107 (2007) 2411–2502.
[2] E.L. Kunkes, D.A. Simonetti, R.M. West, J.C. Serrano-Ruiz, C.A. Gaertner, J.A. Dumesic, Science 322 (2008) 417–421.
[3] M. Snare, I. Kubickova, P. Maki-Arvela, K. Eranen, D. Yu Murzin, Ind. Eng. Chem. Res. 45 (2006) 5708–5715.
[4] H. Bernas, K. Eranen, I. Simakova, A.-R. Leino, K. Kordas, J. Myllyoja, P. Maki-Arvela, T. Salmi, D. Yu, Murzin. Fuel 89 (2010) 2033–2039.
[5] J.G. Immer, M.J. Kelly, H.H. Lamb, Appl. Catal. A 375 (2010) 134–139.
[6] P.T. Do, M. Chiappero, L.L. Lobban, D. Resasco, Catal. Lett. 130 (2009) 9–18.
[7] M. Arend, T. Nonnen, W.F. Hoelderich, J. Fischer, J. Groos, Appl. Catal. A 399 (2011) 198–204.
[8] L. Yang, K.L. Tate, J.B. Jasinski, M.A. Carreon, ACS Catal. 5 (2015) 6497–6502.
[9] S. Popov, S. Kumar, Energy Fuels 29 (2015) 3377–3384.
[10] A. Dragu, S. Kinayyigit, E.J. García-Suárez, M. Florea, E. Stepan, S. Velea, L. Tanase, V. Collière, K. Philippot, P. Granger, V.I. Parvulescu, Appl. Catal. A 504 (2015) 81–91.
[11] M. Ahmadi, A. Nambo, J.B. Jasinski, P. Ratnasamy, M.A. Carreon, Catal. Sci. Technol. 5 (2015) 380–388.
[12] M.A. Alotaibi, E.F. Kozhevnikova, I.V. Kozhevnikov, J. Catal. 293 (2012) 141–144.
[13] M.A. Alotaibi, E.F. Kozhevnikova, I.V. Kozhevnikov, Chem. Commun. 48 (2012) 7194–7196.
[14] K. Alharbi, E.F. Kozhevnikova, I.V. Kozhevnikov, Appl. Catal. A 504 (2015) 457–462.
[15] K. Alharbi, W. Alharbi, E.F. Kozhevnikova, I.V. Kozhevnikov, ACS Catal. 6 (2016) 2067–2075.
[16] S. Itagaki, N. Matsuhashi, K. Taniguchi, K. Yamaguchi, N. Mizuno, Chem. Lett. 43 (2014) 1086–1088.
[17] S. Zhu, X. Gao, Y. Zhu, Y. Zhu, X. Xiang, C. Hu, Y. Li, Appl. Catal. B 140–141 (2013) 60–67.
[18] C. Hoang-Van, G. Tournier, S.J. Teichner, J. Catal. 86 (1984) 210–214.
[19] G.J. Hutchings, Chem. Commun. (2008) 1148–1164.
[20] K.Q. Sun, Y.C. Hong, G.R. Zhang, B.Q. Xu, ACS Catal. 1 (2011) 1336–1346.
[21] D. Tongsakul, S. Nishimura, K. Ebitani, ACS Catal. 3 (2013) 2199–2207.
[22] K. Sun, A.R. Wilson, S.T. Thompson, H.H. Lamb, ACS Catal. 5 (2015) 1939–1948.
[23] Y.F. Han, J.H. Wang, D. Kumar, Z. Yan, D.W. Goodman, J. Catal. 232 (2005) 467–475.
[24] E.K. Hanrieder, A. Jentys, J.A. Lercher, J. Catal. 333 (2016) 71–77.
[25] J. Xu, T. White, P. Li, C. He, J. Yu, W. Yuan, Y.F. Han, J. Am. Chem. Soc. 132 (2010) 10398–10406.
[26] L.B. Ortiz-Soto, O.S. Alexeev, M.D. Amiridis, Langmuir 22 (2006) 3112–3117.
[27] R.N. Singh, R. Awasthi, C.S. Sharma, Int. J. Electrochem. Sci. 9 (2014) 5607–5639.
[28] B. Coq, F. Figueras, J. Mol. Catal. A 173 (2001) 117–134.
[29] F. Gao, D.W. Goodman, Chem. Soc. Rev. 41 (2012) 8009–8020.
[30] Y. Izumi, M. Ono, M. Kitagawa, M. Yoshida, K. Urabe, Microporous Mater. 5 (1995) 255–262.
[31] J.E. Benson, M. Boudart, J. Catal. 4 (1965) 704–710.
[32] J.E. Benson, H.S. Hwang, M. Boudart, J. Catal. 30 (1973) 146–153.
[33] M.R.H. Siddiqui, S. Holmes, H. He, W. Smith, E.N. Coker, M.P. Atkins, I.V. Kozhevnikov, Catal. Lett. 66 (2000) 53–57.
[34] I.V. Kozhevnikov, S. Holmes, M.R.H. Siddiqui, Appl. Catal. A 214 (2001) 47–58.
[35] W. Knaeble, R.T. Carr, E. Iglesia, J. Catal. 319 (2014) 283–296.
[36] T. Pinto, P. Arquilliere, G.P. Niccolai, F. Lefebvre, V. Dufaud, N. J. Chem. 39 (2015) 5300–5308.
[37] P. Claus, Appl. Catal. A 291 (2005) 222–229.
[38] A.S.K. Hashmi, Chem. Rev. 107 (2007) 3180–3211.
[39] T. Okuhara, H. Watanabe, T. Nishimura, K. Inumaru, M. Misono, Chem. Mater. 12 (2000) 2230–2238.
[40] M.A. Alotaibi, E.F. Kozhevnikova, I.V. Kozhevnikov, Appl. Catal. A 447–448 (2012) 32–40.
[41] E. Bus, J.A. van Bokhoven, Phys. Chem. Chem. Phys. 9 (2007) 2894–2902.
[42] R.A. van Santen, M. Neurock, in: G. Ertl, H. Knözinger, F. Schüth, J. Weitkamp (Eds.), Handbook of Heterogeneous Catalysis, vol. 3, Wiley-VCH, 2008, p. 1415.